ORIGINAL PAPER

A probabilistic tsunami hazard assessment for the Makran subduction zone at the northwestern Indian Ocean

Mohammad Heidarzadeh · Andrzej Kijko

Abstract A probabilistic tsunami hazard assessment is performed for the Makran subduction zone (MSZ) at the northwestern Indian Ocean employing a combination of probability evaluation of offshore earthquake occurrence and numerical modeling of resulting tsunamis. In our method, we extend the Kijko and Sellevoll's (1992) probabilistic analysis from earthquakes to tsunamis. The results suggest that the southern coasts of Iran and Pakistan, as well as Muscat, Oman are the most vulnerable areas among those studied. The probability of having tsunami waves exceeding 5 m over a 50-year period in these coasts is estimated as 17.5%. For moderate tsunamis, this probability is estimated as high as 45%. We recommend the application of this method as a fresh approach for doing probabilistic hazard assessment for tsunamis. Finally, we emphasize that given the lack of sufficient information on the mechanism of large earthquake generation in the MSZ, and inadequate data on Makran's paleo and historical earthquakes, this study can be regarded as the first generation of PTHA for this region and more studies should be done in the future.

Keywords Probabilistic tsunami hazard assessment (PTHA) · Seismic hazard analysis · Numerical modeling · Makran subduction zone (MSZ) · Indian Ocean

1 Introduction

In the aftermath of the 2004 Sumatra–Andaman earthquake and tsunami, considerable efforts were made to assess tsunami hazards for vulnerable coastlines throughout the world, mostly using either probabilistic or deterministic methods. Although the deterministic methods have been used for tsunami hazards assessment for several decades, the probabilistic ones are relatively young and still more studies should be conducted in this field.

M. Heidarzadeh (✉)
Department of Civil Engineering, Faculty of Engineering, Tarbiat Modares University, Tehran, Iran
e-mail: heidarz@ut.ac.ir

A. Kijko
Aon Benfield Natural Hazard Centre, University of Pretoria, Pretoria, South Africa

🖉 Springer

In recent years, motivated by the 2004 Indian Ocean mega-tsunami, different algorithms were proposed for probabilistic tsunami hazard assessment (PTHA). As many uncertainties are associated with the modeling of tsunami generation, propagation and runup (Geist and Parsons 2006), probabilistic tsunami hazard assessment is a relatively difficult task compared to deterministic hazard assessment. Despite this, probabilistic methods are important for tsunami hazard assessments as they are the only methods that give the tsunami probabilities.

In this study, we apply a fresh probabilistic method to investigate the likelihood of tsunami in the Makran subduction zone (MSZ) at the northwestern Indian Ocean. MSZ extends east from the Strait of Hormoz in Iran to near Karachi in Pakistan with the length of about 900 km (Fig. 1). It has generated the deadliest known tsunami in the Indian Ocean region prior to 2004, i.e. the Makran tsunami of 1945, with a death toll of about 4000 (Heck 1947). This subduction zone is formed by the northward subduction of the Arabian plate beneath the Eurasian one. A summary of the Makran's tectonic settings and boundaries is shown in Fig. 1. In view of tsunami hazard assessment, Makran remains one of the least studied regions in the world. Nevertheless, Okal and Synolakis (2008) and Heidarzadeh et al. (2008, and 2009) recently studied historical tsunamis and presented preliminary tsunami hazard assessment for this region using deterministic methods (Fig. 1). Here, we further extend these efforts and calculate the probabilities of tsunami occurrence in this region. Our probabilistic tsunami hazard assessment method is based on the Kijko and Sellevoll's (1992) algorithm for seismic hazard assessment. In the following, the details of this method and the results will be presented.

2 Review of international efforts in the field of PTHA

Compared to seismic hazard assessment, probabilistic tsunami hazard analysis (PTHA) is relatively new and few studies exist (e.g., Geist and Parsons 2006). This is in part because
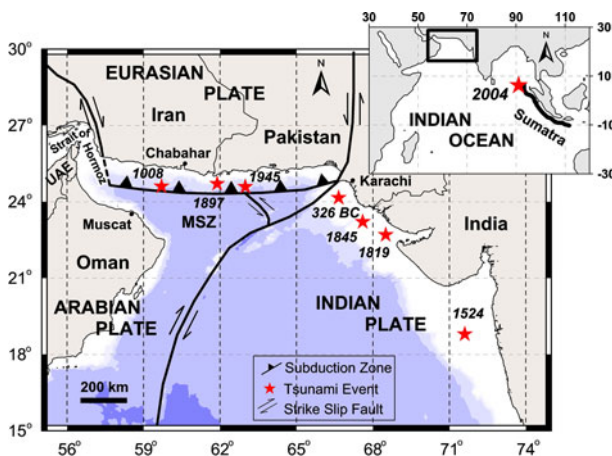
Fig. 1 Two main tsunamigenic sources in the Indian Ocean including Sumatra subduction zone and Makran subduction zone (*top-right*) along with tectonic map of the Makran and its historical tsunamis (*bottom-left*). MSZ stands for the Makran subduction zone

of many uncertainties associated with tsunami events that make it difficult to reliably take them into account and in part because of the importance of tsunami hazard assessment was not well understood before the giant 2004 Sumatra tsunami. Nevertheless, probabilistic methods should be developed further for tsunami engineering because in view of engineering purposes, determining the likelihood of a tsunami with certain wave height is key in any tsunami mitigation program. There are two types of PTHA:

2.1 Modeling-based PTHA

Lin and Tung (1982) suggested that tsunami hazard can be calculated quantitatively in a way similar to seismic hazard analysis. They combined simple seismological and hydrodynamic models and analyzed tsunami hazard as the probability of water elevation exceeding a certain height at a given site. Rikitake and Aida (1988) used the same methodology and employed an improved hydrodynamic model to assess the tsunami hazard probability in Japan. This method also has been applied by other authors (e.g. Geist and Parsons 2006; and Annaka et al. 2007; Burbidge et al. 2008). In modeling-based PTHA, at first most important tsunamigenic zones in the region will be recognized based on the historical data, and then the probability for earthquake occurrence in each zone will be estimated. The possible tsunami from each zone will be modeled in the next step. Finally, the result of PTHA is the product of the earthquake and tsunami probabilities. Figure 2a presents the results of a modeling-based PTHA performed by Annaka et al. (2007) for a coastal site around Japan. As shown in this figure (left panel), the annual probability for this site being hit by a tsunami wave having height equal or larger than 3.6 m is around 0.0015.
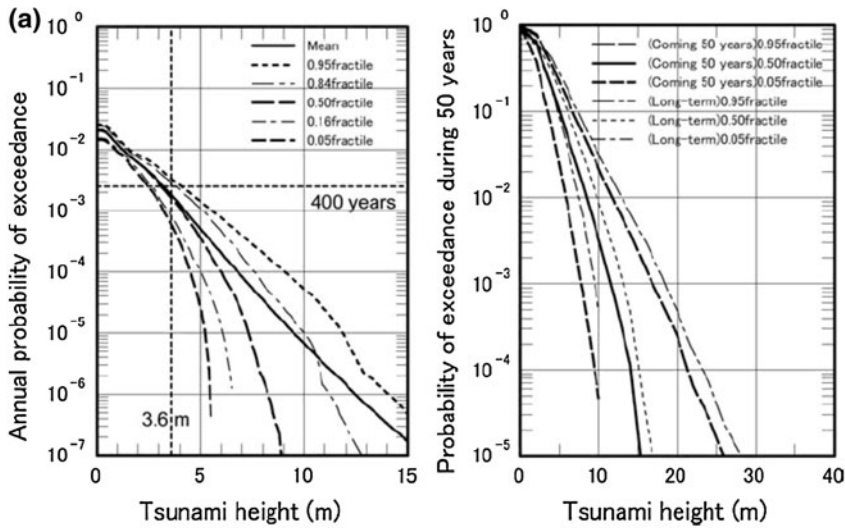
2.2 Runup data-based PTHA

An alternative approach is to examine the past record of tsunami at individual locations and determine whether a scaling relationship describes the record or not (Burroughs and Tebbens 2005). Using runup data from 10 locations in Japan, Burroughs and Tebbens (2005) examined the cumulative frequency-size distributions and determined the scaling relationships and recurrence intervals for runup heights. It is evident that the runup data-based PTHA is applicable only when adequate historical information and measurements of tsunami runup are available. An example of this type of PTHA is shown in Fig. 2b based on the tsunami runup heights at ten locations in Japan performed by Burroughs and Tebbens (2005). Based on these data, power-law scaling relationship in the form of $N_{\mathrm{T}}^{\bullet}(r) = C(r^{-\alpha} - r_{\mathrm{T}}^{-\alpha})$ was used to predict the runup heights, where $N_{\mathrm{T}}^{\bullet}(r)$ is the number of objects per unit time with size greater than or equal to r, α is the scaling exponent, and C is the activity level, a constant equal to the number of objects with size $r \geq 1$. According to cure fits presented in Fig. 2b, the constants α and C are calculated that are shown at the top-right corner of the figure.
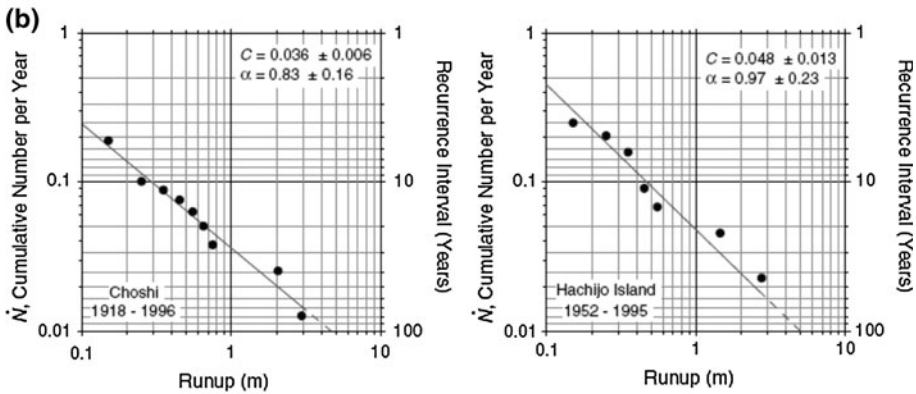
The method that we apply here for PTHA is essentially of the modeling-based type whose detail will be discussed in the following.

3 The present methodology for the MSZ

The historical data of Makran tsunamis is rather poor, and only one tsunamigenic earthquake (the 1945 event) is instrumentally recorded in this region. Therefore, it is clear that

Fig. 2 Examples of modeling-based PTHA (*top panel*, after Annaka et al. 2007), and runup data-based PTHA (*bottom panel*, after Burroughs and Tebbens 2005)

using historical runup data for a PTHA cannot yield useful results, and thus we employ the modeling-based method.

The principals of the method that we apply here for PTHA are similar to other available probabilistic methods, i.e. it contains different tsunami scenarios from different source zones in which every tsunamigenic earthquake has its own weight and that the total tsunami probability in any selected coastline is calculated by considering all tsunami-generating sources in the region. This method is based on a combination of probability evaluation for offshore earthquake occurrence and numerical modeling of tsunami. For numerical modeling of tsunami, we employ a well-validated hydrodynamic model per international standards (Synolakis et al. 2008). This model that is known as TUNAMI-N2 (Tohoku University's Numerical Analysis Model for Investigation of tsunamis-version N2) solves the nonlinear shallow water equations using leap frog scheme of finite

differences. Further information about the numerical model will be presented in the following sections.

The method that we use in this study for probabilistic tsunami hazard assessment (PTHA) includes the following three steps:

(1) Assessment of seismic hazard parameters for the MSZ using the algorithm by Kijko and Sellevoll (1992).
(2) Numerical modeling of tsunamis using TUNAMI-N2 numerical code which is one of the only two existing nonlinear shallow water codes validated with laboratory and field data.
(3) Probabilistic tsunami hazard assessment.
   Sections 4 to 6 will provide more detailed descriptions of each of these steps.

4 Probabilistic forecast of seismic hazard and validation

As the occurrence of a large earthquake in offshore region is necessary for tectonic tsunami generation, the first step in the modeling-based PTHA is to evaluate the probability of offshore earthquake occurrence. This probability often assumes that the frequency of seismic events follows the Gutenberg–Richter (GR) relation (Gutenberg and Richter 1954):

$$\text{Log}_{10}N = a - bM \tag{1}$$

where N is the cumulative total number of earthquakes with magnitude equal to or greater than M that occur in a given region within a certain time period, and a and b are constant parameters that depend on the region. Our region comprised a rectangular area as set out by the coordinates 23–28°N, and 57–70°E (Fig. 3-top). Table 1 provides a list consisting of all the large earthquakes in MSZ where the magnitude estimates were greater or equal to 6.5. As listed in Table 1, the region experienced 8 large historical earthquakes (rows 1–8 in Table 1) with intensities larger than 8. Based on the geographical locations of these historical earthquakes shown in Fig. 1, it can be seen that they are distributed all along the MSZ.

A variety of sources was used to compile an earthquake catalog for the MSZ, including both historical (non-instrumental) and modern (instrumental) events. Data for earthquakes that took place prior to 1900 are referred to as "historical" where "modern" data consist of hypocenters and instrumentally recorded arrival times from worldwide stations as reported in various catalogs, books and journals. For this study, a total number of about 453 earthquakes were used which are shown in Fig. 3-top. As indicated by Table 1, the maximum observed earthquake was the event of the November 27, 1945 with a moment magnitude of 8.1. Figure 3-bottom presents the G–R relation for the MSZ using the compiled earthquake catalog.

It was assumed that the earthquake occurrence is a Poisson process, and therefore any data regarding aftershocks were removed from our data using the method proposed by Gardner and Knopoff (1974). In a Poissonian process, events occur continuously and independently in a random manner. According to the fundamentals of Poisson processes, the events should be independent, and thus it is necessary to remove aftershocks from the earthquake catalog as they are dependant to main shocks.

An assessment of the recurrence parameters (a-value, b-value, $M_{\max}$, and corresponding long-term seismic moment rate) for the MSZ was performed by making use of a procedure developed by Kijko and Sellevoll (1992) that is very flexible and provides some attractive
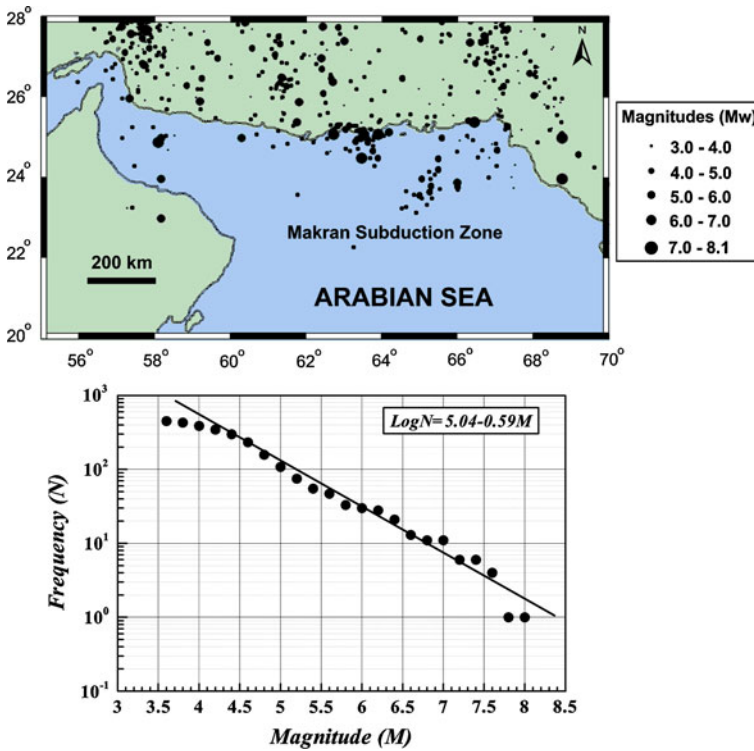
Fig. 3 *Top*: the epicenters and magnitudes of earthquakes in the Makran region (after Heidarzadeh et al. 2008); *Bottom*: the Gutenberg–Richter relation for the seismicity of the MSZ

properties as illustrated in Fig. 4. This figure shows that the Kijko and Sellevoll's (1992) approach accounts for three types of data available in earthquake catalogs which are as follows:

(1) Very strong prehistorical seismic events (paleo-earthquakes), which occurred over the last thousands of years and thus are more likely to have been preserved in the sediment record or historical reports.

(2) The macro-seismic observations of some of the strongest seismic events that occurred over a period of the last few hundred years.

(3) Recent "complete" data for a relatively short period of time.

The "complete" part of the catalog can be divided into several sub-catalogs, each of which is complete for events above a given threshold magnitude $m_{min}^{(i)}$, in a certain period of time T_i where $i = 1,\dots, s$ and s is the number of complete sub-catalogs (Fig. 4).

4.1 Details of the Kijko and Sellevoll's (1992) approach

This approach permits 'gaps' (T_g) (Fig. 4) where records are or maybe missing or when seismic networks were out of operation. In addition, uncertainty in earthquake magnitude is also taken into account. In this context, it is assumed that the observed or inferred

Table 1 A list of Makran historical and instrumental great earthquakes (magnitude ≥6.5)

No.	Date (yy-mm-dd)	Latitude (degree)	Longitude (degree)	Focal depth (km)	Ms[a]	Mw[b]	Intensity (MM)[c]	References[e]
1	326 BC	24.00 N	67.30 E				Strong tsunami was produced	(1,2,3,4)
2	1008-5	25.00 (27.7)[d]	60.00 (52.3)[d]				8–9	(2,3,4,5,6)
3	1483-2-18	24.90	57.90				10	(5,7,8)
4	1668-5	25.00	68.00				8–9	(7,9,10)
5	1688-5	24.00	68.00				8–9	(7,9,10)
6	1765	25.40	65.80				8–9	(8,11)
7	1849	27.70	57.60				8–9	(5,7)
8	1851-4-19	25.10	62.30				8–9	(5,8,10,12,17)
9	1927-07-07	27.00	62.00		6.5			(5,13)
10	1929-09-03	26.40	62.30		6.5			(5,13)
11	1934-06-13	27.43	62.59	35.0	7.0			(5,13)
12	1945-11-27	24.50	63.00	25.0		8.1		(1,2,3,4,5,6,7,8,10,13,14,16,17,18)
13	1947-08-05	25.10	63.40	35.0	7.6			(5,7,8,13)
14	1948-1-30	25.14	63.69	30.0	6.5			(13,9)
15	1962-12-26	23.90	65.40		6.5			(13,9)
16	1964-12-22	27.80	57.00		6.5			(13,9)
17	1969-11-07	27.90	60.10	35.0	6.5			(5,13)
18	1972-08-06	25.40	61.40		7.0			(13,15,9)
19	1974-12-02	24.00	58.00		6.5			(13,9,15)
20	1979-01-10	26.52	61.01		6.7			(13,9,15)
21	1980-11-28	23.00	58.00		7.0			(13,9,15)
22	1983-04-18	27.79	62.05	64.0		7.0		(9,13,15)
23	1990-06-17	27.40	65.72	14.0	7.0			(13,15,9)

[a] Surface Wave Magnitude, [b] Moment Magnitude, [c] Modified Mercalli, [d] Reported by Ambraseys and Melville 1982

[e] (1): Murty and Rafiq (1991); (2) Murty and Bapat (1999); (3) Pararas-Carayannis (2006); (4) Dominey-Howes et al. (2007); (5) Ambraseys and Melville (1982); (6) Rastogi and Jaiswal (2006); (7) NOAA (2007); (8) Byrne et al. (1992); (9) USGS (2007); (10) Quittmeyer and Jacob (1979); (11) Walton (1864); (12) Merewether (1852); (13) ISC (2007); (14) Pendse (1946); (15) Harvard Seismology (2007); (16) Heck (1947); (17) Okal et al. (2006); (18) Berninghausen (1966)
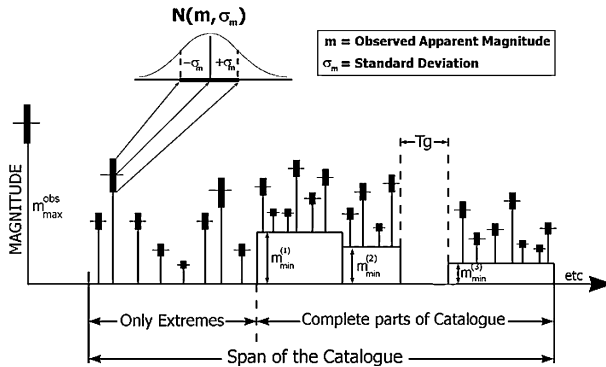
Fig. 4 Illustration of data that can be used to obtain basic seismic hazard parameters for the area in the vicinity of a selected site by the procedure used. m_{max}^{obs} and T_g are the largest known historical earthquake and "gaps" in data, respectively. σ_m and m_{min} are standard deviation and threshold magnitude considered for each sub-catalog (after Kijko and Sellevoll 1992)

earthquake magnitudes are subjected to a random error that follows a Gaussian distribution with zero mean and a known standard deviation. Then, the assumed values of expected errors will be taken into account in hazard analyses.

The joint likelihood function is obtained as the product of the likelihood functions for the extreme and complete sub-catalogs. In addition, the procedure makes it possible to estimate the maximum regional earthquake magnitude, m_{max}, from the largest known earthquake that occurred before the catalog begins.

Assuming that the earthquake magnitudes are distributed according to the doubly truncated frequency–magnitude Gutenberg–Richter relation, the maximum regional magnitude, m_{max}, can be obtained using the following equation:

$$m_{max} = m_{max}^{obs} + \frac{E_1(n_2) - E_1(n_1)}{\beta \exp(-n_2)} + m_{min}\exp(-n), \tag{2}$$

where m_{max}^{obs} is the maximum observed magnitude (M_w 8.1 for the Makran region), n is the number of earthquakes, with a magnitude equal to or exceeding the threshold magnitude m_{min}, $n_1 = n/\{1-\exp[-\beta(m_{max}-m_{min})]\}$, $n_2 = n_1 \exp[-\beta(m_{max}-m_{min})]$, β is related to Gutenberg–Richter parameter b through the relation $\beta = b\ln(10)$ and E_1 denotes an exponential integral function defined as $E_1(z) = \int_z^\infty \exp(-\xi)/\xi d\xi$.

It is important to note that Eq. (2) has several interesting properties (Kijko 2004). For example, it may also be used when the exact number of earthquakes, n, is unknown. In this case, the number of earthquakes, n, can be replaced by λT, where λ is the parameter of the Poisson distribution, and T is the span of the seismic event catalog. Such a replacement is equivalent to the assumption that the number of earthquakes occurring in unit of time conforms to the Poisson distribution with parameters λ and T. It must be noted that in its current form, Eq. (2) does not constitute an estimator for m_{max} since expressions n_1 and n_2, which appear on the right-hand side of the equation, also depends on m_{max}. In the general case, the assessment of m_{max} is obtained by solving Eq. (2) iteratively.

We proceed and divided the catalog of Makran earthquakes into four parts. The first part contains the historical large events (non-instrumental events). The other three parts are "complete" sub-catalogs that include instrumental data. A certain threshold magnitude and a standard deviation were assigned to each sub-catalog. A summary of the details of each

Table 2 Summary of the details of the four parts of the earthquake catalog used for seismic hazard analysis

	Extreme earthquakes	Complete part-1	Complete part-2	Complete part-3	Total
Start time	1000-01-01	1900-01-01	1964-01-01	1990-01-01	
End time	1899-12-31	1963-12-31	1989-12-30	2007-05-06	
Threshold earthquake	4.0	4.0	4.0	4.0	
Error value	±0.5	±0.3	±0.2	±0.1	
No. of earthquakes	7	28	202	216	453

part of the earthquake catalog used for seismic hazard analysis is presented in Table 2. As shown in this table, the threshold earthquake is 4.0 for all of the parts, and the values of random error standard deviation are ranging between ±0.5 and ±0.1.

4.2 Results of probabilistic forecast of seismic hazard and validation

The results of seismic hazard assessment for the MSZ are shown in Fig. 5. Estimates of the earthquake return periods are shown in Fig. 5a. Also, Fig. 5b presents the probability of earthquakes with certain magnitudes over 1, 50, 100 and 1000-year periods. For example, based on Fig. 5, the return period of an M_w 8.1 earthquake is about 250 years in the MSZ, while the probability of having such an earthquake over a 50-year period is about 17.5%. Table 3 presents the results of β and λ values obtained from our seismic hazard analysis along with data contribution to these parameters from each part of the earthquake catalog.

As it was discussed by Heidarzadeh et al. (2008), we compare our results with the previous estimates of the return period of large earthquakes in the MSZ to validate the results of the above seismic hazard assessment. Byrne et al. (1992) have asserted that, if all of the plate motion between Eurasia and Arabia occurred through earthquakes like the 1945 event (M_w 8.1), such events would be expected to repeat in eastern Makran roughly every 175–300 years. Also, Page et al. (1979) estimated that the recurrence of a 1945-like earthquake along the eastern MSZ is ∼125–250 years. Our results presented in Fig. 5a suggest a return period of about 250 years for a 1945-like earthquake (M_w 8.1) in overall good agreement with the earlier estimates.

5 Numerical modeling of tsunami and validation

Different methods such as finite differences, finite elements, finite volumes, and method of characteristics have been used in solution of nonlinear form of shallow water equations for tsunami modeling. Some of the developed models in this field are TUNAMI-N2, MOST, COMCOT, TsunamiCLAW, NAMI DANCE, TsunAWI and others. TUNAMI-N2 that uses finite difference method is one of the valid and verified tsunami numerical models used in scientific and operational purposes. In this study, TUNAMI-N2 is used for simulation of propagation and coastal amplification of long waves. The code was originally authored by Nobuo Shuto and Fumihiko Imamura of the Disaster Control Research Center in Tohoku University, Japan, through the Tsunami Inundation Modeling Exchange (TIME) program (Goto et al. 1997). It solves the nonlinear shallow water equations in Cartesian coordinates using a leap-frog scheme in the finite difference technique for basins of irregular shape and topography (Yalciner et al. 2002). Also, a similar methodology is used
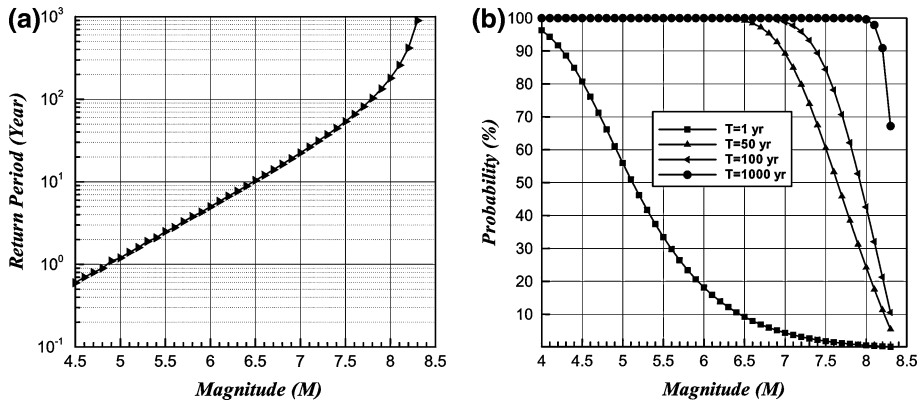
Fig. 5 Estimation of the earthquake return periods in the Makran region (**a**), and the probability of earthquakes with certain magnitudes over 1-, 50-, 100-, and 1000-year periods (**b**) (after Heidarzadeh et al. 2008)

Table 3 Results of beta (β) and lambda (λ) values obtained from seismic hazard analysis and data contribution to these values from ach sub-catalog

	Value	Data contribution (%)				
		Extreme earthquakes	Complete part-1	Complete part-2	Complete part-3	Total
Lambda (λ)	6.58 ± 0.38	2.0	7.1	50.6	40.3	100
Beta (β)	1.38 ± 0.05	39.0	15.5	24.5	21.0	100

in numerical model MOST (Method of Splitting Tsunami) developed by Titov and Synolakis (1998). TUNAMI-N2 and MOST are the only two existing nonlinear shallow water codes validated with laboratory and field data (Yeh et al. 1996).

The algorithm of Mansinha and Smylie (1971) was used to predict seafloor displacement due to an earthquake and to model the initial water displacement. The seismic parameters of the November 27, 1945 earthquake as estimated in the study of Byrne et al. (1992) were used as follows: seismic moment of $1.8 \times 1,021$ N.m, moment magnitude of M_w 8.1, rupture length of 100–150 km, rupture width of about 50–100 km, slip on the fault surface of 6–7 m, strike angle of 246°, dip angle of 7°, slip angle of 89°, and depth of 27 ± 3 km. For our source analysis, the mentioned parameters are as follows: 130 km, 70 km, 6.6 m, 246°, 7°, 89°, and 27 km, respectively.

The total number of grid points in the computational domain was 369852, i.e., a 833×444 grid. The time step was selected as 1.0 s to satisfy the stability condition, and the duration time of wave propagation was 5 h. The 1-min bathymetry data provided through the GEBCO digital atlas was used in this study (IOC et al. 2003). Runup calculations were not included in our numerical modeling, but the maximum positive tsunami heights (amplitudes) along the coast were calculated, which give a reasonable approximation of the runup heights. By comparing the wave height along the coast with actual runup calculations at a particular coastline in the Makran region, Heidarzadeh et al. (2009) showed that it is a reasonable method to estimate runup heights.

To validate the results of numerical modeling of tsunami, Heidarzadeh et al. (2009) modeled the November 27, 1945 earthquake and tsunami, which is the only instrumentally recorded tsunamigenic earthquake in the MSZ, and compared the modeling results with historical observations. According to Heidarzadeh et al. (2009), good agreement was observed between computed and observed wave heights. They showed that the modeling was successful in reproducing 4–5 m wave height in Pasni and 1.5 m wave height in Karachi, which were reported in historical reports. Also, it was shown that the largest wave arrived 120 min after the earthquake in Karachi, which is in approximate agreement with historical observations.

6 Probabilistic tsunami hazard assessment

We estimate probabilistic tsunami risk through a combination of evaluating probabilities of offshore earthquake occurrence and numerical modeling of the resulting tsunami. Based on this method, the probability of having a tsunami with a particular wave height in a selected coastline is calculated using the following equation, which is modified from Rikitake and Aida (1988):

$$P_{tsu}(C_k, Z_i, h_{cr}, M, T) = \begin{cases} P_{eq}(Z_i, M, T) & h_{max}(C_k) \geq h_{cr} \\ 0 & h_{max}(C_k) < h_{cr} \end{cases} \tag{3}$$

where $P_{tsu}(C_k, Z_i, h_{cr}, M, T)$ is the probability of tsunami whose wave height exceeds a certain level (h_{cr}) at a selected kth coastline (C_k) due to an earthquake with magnitude M in the ith tsunamigenic zone (Z_i) in a time interval of T years. $h_{max}(C_k)$ is the maximum calculated tsunami wave height in the selected kth coastline (C_k). Also, $P_{eq}(Z_i, M, T)$ is the probability of an earthquake with magnitude M in the ith tsunamigenic zone (Z_i) in the time interval of T years. Using Eq. (3), the total tsunami probability in any selected coastline is calculated by considering all tsunami-generating sources in the region using Eq. (1) of Rikitake and Aida (1988) as follows:

$$P_{tsu}^T(C_k, Z_i, h_{cr}, M, T) = 1 - \prod_{i=1}^{n} [1 - P_{tsu}(C_k, Z_i, h_{cr}, M, T)] \tag{4}$$

where n is the total number of tsunami-generating sources, and $P_{tsu}^T(C_k, Z_i, h_{cr}, M, T)$ is the total tsunami probability.

Based on the locations of the previous earthquakes and tsunamis in the region, we divided Makran into three tsunami-generating sub-regions including eastern Makran, middle Makran, and western Makran named as Z_1, Z_2, and Z_3, respectively (Fig. 6). The basis for this segmentation is the study by Byrne et al. (1992) who studied Makran's historical large earthquakes. Based on their study, the region was devastated by seven large earthquakes in the past, which ruptured the Makran's plate boundary in four segments; one in the western Makran, two in the middle Makran, and the other in the eastern part.

The data of tsunamigenic earthquakes in the Makran region are poor, and the magnitude of the parent earthquakes is known only for one event, the tsunami of 1945, with a moment magnitude of 8.1. Hence, it is impossible to determine a reasonable magnitude of tsunami-generating earthquakes in each of the above sub-regions from historical data, and thus we assume it to be 8.1 in all three zones, similar to the magnitude of the 1945 event. It should be noted that we further assume that the probability of earthquake occurrence in each zone follows the probability curves presented in Fig. 5 although these curves were obtained for
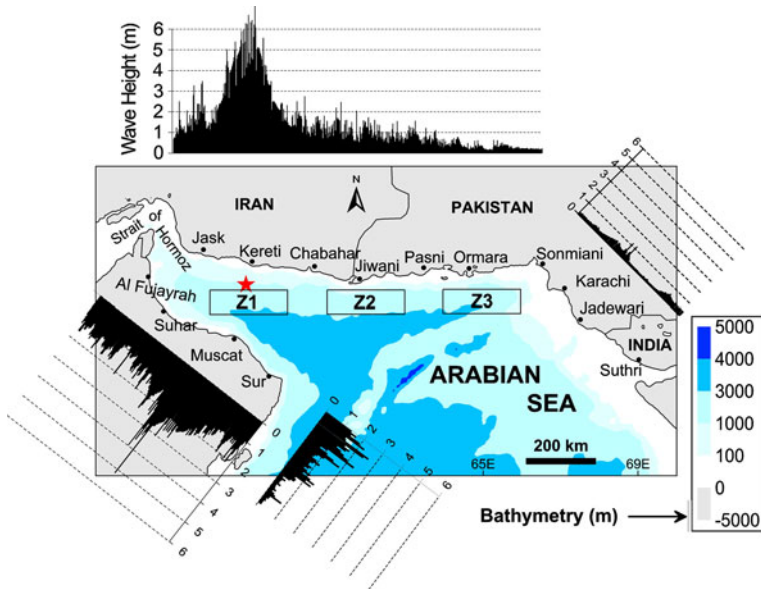
Fig. 6 Three tsunamigenic sub-regions in the MSZ used in this study (Z_1, Z_2, and Z_3) along with the distribution of maximum computed positive tsunami wave heights along various Makran coasts produced by a 1945-like earthquake in the Z_1. The epicenter of the earthquake is shown by a *star*. The map also shows the bathymetry of the northwestern Indian Ocean

the whole region. These assumptions seem reasonable because of the complex nature of the earthquake occurrence in the MSZ. For example, Byrne et al. (1992) reported a strong variation between the seismicity of the western and eastern parts of the MSZ so that the eastern part was seismically more active in the past. As the western Makran did not rupture in large earthquakes in the past 500 years, Quittmeyer and Jacob (1979) concluded that the western Makran could feature a seismic gap that may result in large future earthquakes. Therefore, it can be seen that the pattern of earthquake occurrence in the region is very complicated.

The distribution of tsunami wave heights from these sources along Makran coasts can be calculated; the result for an earthquake in Z_1 is shown in Fig. 6. Examples of tsunami snapshots due to earthquake occurrence in each zone are shown in Fig. 7.

For example, according to the results of seismic hazard assessment (Fig. 5), the probability of having a 1945-like earthquake (*Mw* 8.1) in a 50-year period is about 17.5%. According to Fig. 6, such an earthquake in the eastern Makran (Z_1) may produce offshore wave heights of about 6 m and 1.25 m in Kereti and Chabahar, respectively. Therefore, the probabilities for Kereti being hit by tsunami waves having heights equal to or larger than 1, 3, 5, and 7 m due to a 1945-like earthquake in Z_1 are evaluated as 0.175, 0.175, 0.175, and 0, respectively, for a 50-year period. The respective probabilities for Chabahar are 0.175, 0, 0, and 0, respectively. It should be noted that wave heights of 1, 3, 5, and 7 m used above for calculating tsunami probabilities, represent small (1 m wave height), medium (3 and 5 m wave height), and large tsunamis (7 m wave height), respectively.

Table 4 presents tsunami wave heights due to different source scenarios at selected coastal locations along with probabilities of tsunami wave exceeding the key heights at selected coastal locations in a 50-year period. As can be seen in this table, the probability
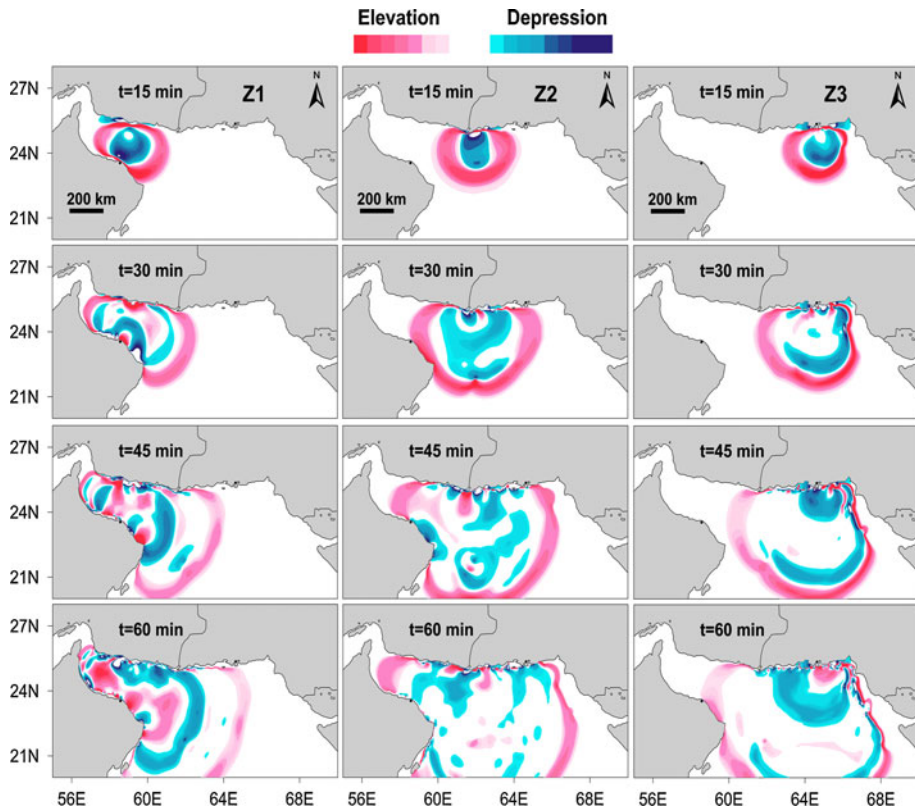
Fig. 7 Snapshots of tsunami simulations at times t = 15, 30, 45, and 60 min due to a 1945-like earthquake in Z_1 (*left column*), Z_2 (*middle column*), and Z_3 (*right column*)

of having a tsunami wave exceeding 5 m of height in Jiwani over the next 50 year is 17.5%.

Similar probability evaluations are made for different coastlines in the northwestern Indian Ocean as shown in Fig. 8. This figure shows that the northern coast of Makran, i.e. the southern coasts of Iran and Pakistan, experience the largest tsunami waves. It is observed from this figure that the area with the highest probability of a tsunami wave exceeding 5 m is expected in the southern coasts of Iran and Pakistan. Most shorelines along these coasts are characterized by a probability of 17.5% for tsunami waves exceeding 3 m over a 50-year period (Fig. 8).

In northern Oman, the probability of tsunami waves exceeding 5 m is negligible for approximately the entire coast, whereas the areas adjacent to Muscat experience relatively large tsunami amplitudes of larger than 5 m resulting in 17.5% probability over a 50-year period. It therefore can be concluded that the southern coasts of Iran and Pakistan as well as Muscat are at highest risk. Wave amplification can be observed in Karachi, although the maximum wave amplitude is about 2 m (Fig. 8). While the probabilities of waves exceeding 1 and 2 m are negligible for many adjacent areas, they are about 32 and 18%, respectively, in Karachi.

According to Fig. 8, the highest probability for moderate tsunamis ($1 \leq h < 2$ m) is again expected from southern coasts of Iran and Pakistan as well as southern coasts of

Table 4 Tsunami wave heights due to different source scenarios along with probabilities of tsunami wave exceeding the key heights at selected coastal locations in a 50-year period

Coastal locations	Longitude (°E)	Latitude (°N)	Wave height due to different source zones (m)			Probability of tsunami wave exceeding key heights (%)		
			Z_1	Z_2	Z_3	≥ 1	≥ 3	≥ 5
Jask	57.77	25.63	3.49	0.67	0.22	17.50	17.50	0.00
Kereti	59.08	25.45	4.54	0.50	0.24	17.50	17.50	0.00
Chabahar	60.62	25.28	1.42	2.19	0.38	31.94	0.00	0.00
Jiwani	61.75	25.00	1.28	5.27	1.12	43.85	17.50	17.50
Pasni	63.45	25.27	0.49	1.15	0.88	17.50	0.00	0.00
Ormara	64.62	25.22	0.20	0.45	2.49	17.50	0.00	0.00
Sonmiani	66.58	25.42	0.23	0.47	1.69	17.50	0.00	0.00
Karachi	67.00	24.85	0.57	1.12	1.95	31.94	0.00	0.00
Jadewari	67.58	24.00	0.11	0.19	0.38	0.00	0.00	0.00
Suhar	56.70	24.35	1.48	0.45	0.18	17.50	0.00	0.00
Muscat	58.53	23.60	3.04	0.56	0.28	17.50	17.50	0.00
Sur	59.55	22.55	1.33	0.55	0.21	17.50	0.00	0.00

Oman with a probability of about 45% over a 50-year period (Fig. 8). It is clear that there is a high probability for moderate tsunamis in all Makran coasts that emphasizes the urgent need for the development of a regional tsunami warning system in the region. There is also an urgent need for educating local residents on tsunami hazards, as already is underway in some parts of the world (Synolakis and Bernard 2006).

7 Discussions

For several reasons, we believe that this study should be regarded as the first generation of PTHA for the Makran region. First, the December 26, 2004 Indian Ocean earthquake and tsunami showed that the mechanism of large earthquake generation in the world's subduction zones is very complicated, and it may take several centuries to understand its pattern (McCaffrey 2007). Second, the data on the historical and paleo-earthquakes in the Makran region are poor as the communities along the Makran coasts were small even today due to its very dry climate and little rainfall (Byrne et al. 1992), whereas in other tsunamigenic regions in the world, e.g., Japan, Italy and Greece, the earthquake and tsunami data span over hundreds to thousands of years. Therefore, it is just a reasonable engineering assumption that we assumed that the moment magnitude of a tsunami-generating earthquake is 8.1 in the region.

In this study, based on the previous tsunami data, we determined a single moment magnitude for tsunami-generating earthquake for each sub-region and then calculated the tsunami probabilities. In other words, a single curve was presented as the final result of our PTHA for the Makran (Fig. 8). However, some authors (e.g., Burbidge et al. 2008) varied the earthquake magnitude and presented different curves of tsunami probability to account for different levels of earthquakes. Also, one can use a finite range of earthquake magnitude to obtain a single hazard curve. Here, for PTHA of the MSZ, we preferred not to develop different hazard curves because it may be difficult for the hazard authorities to
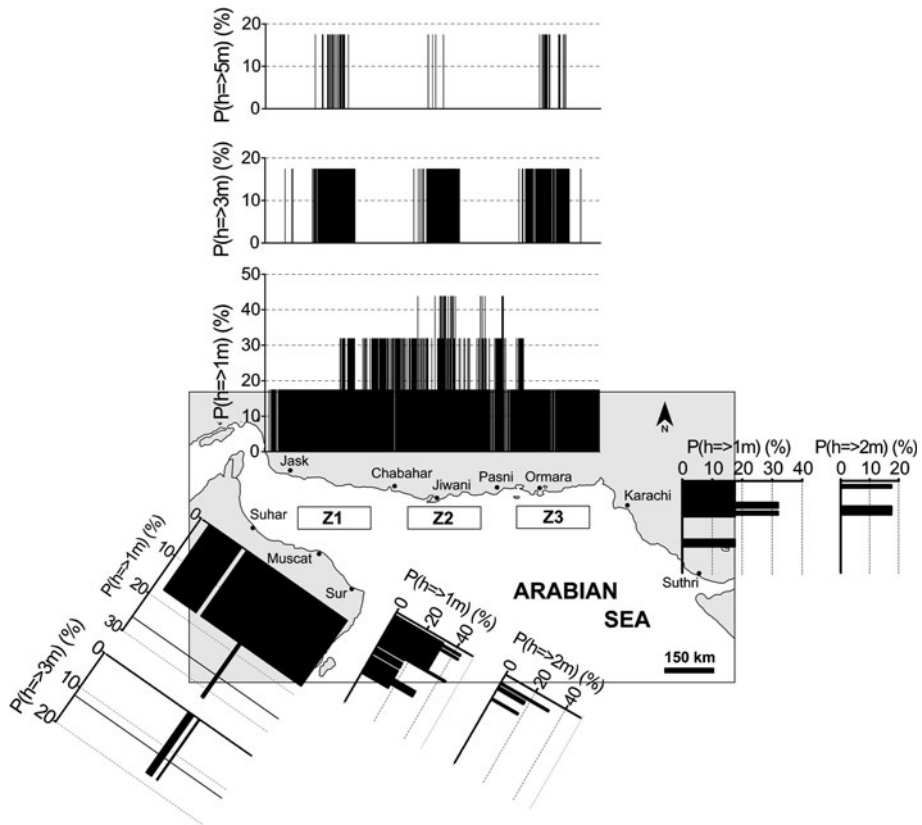
Fig. 8 Probabilities for the coastal areas of the northwestern Indian Ocean being hit by tsunami waves exceeding 1, 2, 3, and 5 m over a 50-year period

interpret and effectively use them as the tsunami hazard understanding in this region is not sufficient. Despite this, the same methodology can be used to develop different hazard curves in the future if needed.

8 Conclusion

We conducted a probabilistic tsunami hazard assessment for the Makran region. The main findings are as follows:

(1) In our probabilistic method for tsunami hazard assessment, we extended the Kijko and Sellevoll's (1992) probabilistic analysis from earthquakes to tsunamis. This application greatly simplified the relatively difficult task of doing PTHA, and thus we recommend this method as a fresh approach for doing probabilistic hazard assessment for tsunamis.

(2) It has been observed that the southern coasts of Iran and Pakistan are extremely vulnerable areas and may experience wave heights larger than 5 m, for a 1945-like tsunamigenic earthquake. The probability of having tsunami waves exceeding 5 m over a 50-year period in these coasts is 17.5%.

(3) Wave heights exceeding 5 m are expected in Muscat, with the probability of 17.5% over a 50-year period. Strong wave amplification is evident in areas adjacent to Muscat.

(4) The highest probability for moderate tsunamis ($1 \leq h < 2$ m) is expected from southern coasts of Iran and Pakistan, as well as the southern coast of Oman with a probability of about 45% over a 50-year period.

(5) We emphasize that given the lack of sufficient information on the mechanism of large earthquake generation in the MSZ, and inadequate data on Makran's paleo and historical earthquakes, this study can be regarded as the first generation of PTHA for this region, and more studies should be done in the future.

Based on the results, the first priority for tsunami hazard mitigation planning in the region should be given to the development of inundation maps for the southern coasts of Iran and Pakistan and Muscat. The development of a regional tsunami warning system in the Makran zone as well as public education on tsunami hazards is of the utmost importance.

References

Ambraseys NN, Melville CP (1982) A history of Persian earthquakes. Cambridge University Press, Britain

Annaka T, Satake K, Sakakiyama T, Yanagisawa K, Shuto N (2007) Logic-tree approach for probabilistic tsunami hazard analysis and its applications to the Japanese coasts. Pure Appl Geophys 164:577–592

Berninghausen WH (1966) Tsunamis and seismic seiches reported from regions adjacent to the Indian Ocean. Bull Seismol Soc Am 56(1):69–74

Burbidge D, Cummins PR, Mleczko R, Thio H (2008) A probabilistic tsunami hazard assessment for Western Australia. Pure Appl Geophys 165:2059–2088

Burroughs SM, Tebbens SF (2005) Power-law scaling and probabilistic forecasting of tsunami runup heights. Pure Appl Geophys 162:331–342

Byrne DE, Sykes LR, Davis DM (1992) Great thrust earthquakes and aseismic slip along the plate boundary of the Makran subduction zone. J Geophys Res 97(1B):449–478

Dominey-Howes D, Cummins P, Burbidge D (2007) Historic records of teletsunami in the Indian Ocean and insights from numerical modeling. Nat Hazards 42(1):1–17

Gardner JK, Knopoff L (1974) Is the sequence of earthquakes in southern California, with aftershocks removed, Poissonian? Bull Seismol Soc Am 64:1363–1368

Geist EL, Parsons T (2006) Probabilistic analysis of tsunami hazards. Nat Hazards 37:277–314

Goto C, Ogawa Y, Shuto N, Imamura F (1997) Numerical method of tsunami simulation with the leap-frog scheme. (IUGG/IOC Time Project), IOC Manual, UNESCO, No. 35

Gutenberg B, Richter CF (1954) Seismicity of the earth and associated phenomena, 2nd edn. Princeton University Press, NJ, USA

Harvard Seismology (2007) Global CMT catalog search, www.globalcmt.org. Harvard University, Cambridge, MA, USA

Heck NH (1947) List of seismic sea wave. Bull Seismol Soc Am 37(4):269–286

Heidarzadeh M, Pirooz MD, Zaker NH, Synolakis CE (2008) Evaluating tsunami hazard in the northwestern Indian Ocean. Pure Appl Geophys 165(11–12):2045–2058

Heidarzadeh M, Pirooz MD, Zaker NH, Yalciner AC (2009) Preliminary estimation of the tsunami hazards associated with the Makran subduction zone at the northwestern Indian Ocean. Nat Hazards 48(2):229–243

International Seismological Centre (ISC) (2007) On-line bulletin, http://www.isc.ac.uk. International Seismological Centre, Thatcham, UK

IOC, IHO, BODC (2003) Centenary edition of the GEBCO digital atlas, published on CD-ROM on behalf of the Intergovernmental Oceanographic Commission and the International Hydrographic Organization as part of the general bathymetric chart of the oceans. British Oceanographic Data Centre, Liverpool

Kijko A (2004) Estimation of the maximum earthquake magnitude m_{max}. Pure Appl Geophys 161:1655–1681

Kijko A, Sellevoll MA (1992) Estimation of earthquake hazard parameters from incomplete data files. Part II: incorporation of magnitude heterogeneity. Bull Seismol Soc Am 82(1):120–134

Lin IC, Tung CC (1982) A preliminary investigation of tsunami hazard. Bull Seismol Soc Am 72(6):2323–2337

Mansinha L, Smylie DE (1971) The displacement field of inclined faults. Bull Seismol Soc Am 61(5):1433–1440

McCaffrey R (2007) The next great earthquake. Science 315:1675–1676

Merewether W (1852) A report of the disastrous consequences of the severe earthquake felt in the provinces of Upper Scinde on the 24th January 1852. J Bombay Geogr Soc 10:284–286

Murty T, Bapat A (1999) Tsunamis on the coastlines of India. Sci Tsunami Hazards 17(3):167–172

Murty T, Rafiq M (1991) A tentative list of tsunamis in the marginal seas of the north Indian Ocean. Nat Hazards 4:81–83

National Oceanic and Atmospheric Administration (NOAA) (2007) National Geographical Data Center (NGDC), www.ngdc.noaa.gov. NOAA, Washington DC, USA

Okal EA, Synolakis CE (2008) Far-field tsunami hazard from mega-thrust earthquakes in the Indian Ocean. Geophys J Int 172(3):995–1015

Okal EA, Fritz HM, Raad PE, Synolakis CE, Al-Shijbi Y, Al-Saifi M (2006) Oman field survey after the December 2004 Indian Ocean Tsunami. Earthq Spectra 22(S3):S203–S218

Page WD, Alt JN, Cluff LS, Plafker G (1979) Evidence for the recurrence of large-magnitude earthquakes along the Makran coast of Iran and Pakistan. Tectonophysics 52:533–547

Pararas-Carayannis G (2006) The potential for tsunami generation along the Makran subduction zone in the northern Arabian Sea. Case study: the earthquake and tsunami of November 28, 1945. Sci Tsunami Hazards 24(5):358–384

Pendse CG (1946) The Mekran earthquake of the 28th November 1945. India Meteorol Depart Sci Notes 10(125):141–145

Quittmeyer RC, Jacob KH (1979) Historical and modem seismicity of Pakistan, Afghanistan, northwestern India, and southeastern Iran. Bull Seismol Soc Am 69(3):773–823

Rastogi BK, Jaiswal RK (2006) A catalog of tsunamis in the Indian Ocean. Sci Tsunami Hazards 25(3):128–143

Rikitake T, Aida I (1988) Tsunami hazard probability in Japan. Bull Seismol Soc Am 78(3):1268–1278

Synolakis CE, Bernard EN (2006) Tsunami science before and beyond boxing day 2004. Philos Trans Royal Soc A 364:2231–2265

Synolakis CE, Bernard EN, Titov VV, Kanoglu U, Gonzalez FI (2008) Validation and verification of tsunami numerical models. Pure Appl Geophys 165(11–12):2197–2228

Titov VV, Synolakis CE (1998) Numerical modeling of tidal wave runup. J Waterway, Port, Costal, Ocean Eng B124:157–171

US Geological Survey (USGS) (2007) USGS National Earthquake Information Center (NEIC), http://www.usgs.gov. US Geological Survey, Washington DC, USA

Walton HI (1864) Transactions of the Bombay geographical society from January 1863 to December 1864. Education Society's Press, Byculla, India

Yalciner AC, Alpar B, Altinok Y, Ozbay I, Imamura F (2002) Tsunamis in the Sea of Marmara, historical documents for the past, models for the future. Mar Geol 190:445–463

Yeh H, Liu P, Synolakis CE (1996) Long wave runup models. World Scientific Publication Company, London 403 pp